Establishment Times of Hypersonic Shock-Wave Boundary-Layer Interactions in Intermittent Facilities

Leon Vanstone*

The University of Texas at Austin, Austin, TX 78724

David Estruch-Samper†

National University of Singapore, Singapore

Bharathram Ganapathisubramani‡

University of Southampton, UK

This study examines establishment times of shock-wave boundary-layer interactions across a range of interaction types and intermittent facilities. Successful design of a test-article for a short duration facility is difficult, especially when trying to guarantee establishment of the flow. While this study does not detail design methodologies of a test article it does aim to provide better understanding of establishment metrics and predictive methods that have emerged from other studies in order to help in the design and assessment of experiments. Experimental and numerical data was taken at Mach 8.9 on an axisymmetric blunt-nosed body with an eight degree flare and laminar boundary-layer. It is shown that the global applicability of any single metric is poor and hence an establishment criteria is developed for this study which provides a more global metric of establishment. Further, a framework is provided for when the use of existing establishment metrics is appropriate.

I. Introduction

Achieving accurate experimental hypersonic results is challenging, not least due to the low tunnel run times experienced with intermittent hypersonic facilities. This study is concerned with the establishment times of these high-speed hypersonic facilities, particularly in relation to shock-wave boundary-layer interactions (SWBLIs).

In continuous (long duration) facilities, the freestream test-flow is established and runs for many characteristic flow times, establishment of the phenomenon in question is of little concern as it is possible to wait to ensure establishment before taking data. However, intermittent (short duration) facilities run for extremely limited periods of time. It is well documented that characteristic time-scales within the re-circulation bubble of a shock-induced boundary-layer

*Research Fellow, The University of Texas at Austin, USA vanstone@utexas.edu

†Assistant Professor, National University of Singapore, Singapore

‡Professor, University of Southampton, UK

separation are considerably larger than those of the outboard flow. In a short duration facility it is entirely possible to have an established (steady) freestream test-flow but have a SWBLI within that is not established and, potentially, never establishes before the end of the steady freestream test-flow conditions. Obvious problems arise when measuring a phenomena which might not be established. Hence, serious concern is given to ensuring that the SWBLI being generated is established within the freestream steady-run window while still providing enough time to take measurements.

It is important to note that establishment of a SWBLI is strongly dependent on the design of the experiment. Given the expense associated with model manufacture and running intermittent facilities, trial and error is usually not an acceptable method of ensuring establishment. Normally, some provisional investigation is required to help guide the design of the final test article, which is then assessed to ensure establishment.

Early studies were relatively rigorous in examining establishment of experiments within intermittent facilities [1, 2]. Knowledge of establishment times was very limited and significant effort was expended to ensure the tunnel flow would be established before a model was made. As experience with these types of facilities increased further studies emerged which proposed analytical or empirical relationships associated with establishment of certain facility/model types [3]. These models attempted to scale existing establishment times using different empirically or analytically derived parameters such as flow times [4, 5] or flow lengths [6]. Establishment of the tunnel flow assessed in this manner was based on trends extracted across previous studies which all featured relatively detailed establishment studies.

More recent studies have a tendency of justifying establishment of their experiments through the various empirical/analytical metrics and scaling parameters that have evolved from these previous experiments. It is often unclear to what extent establishment of the chosen experimental geometry has been examined and to what degree it relies on previous results.

One possible solution to these issues comes from recent advances in computational power which has seen the emergence of numerical solvers that should be capable (when time accurate) of also providing estimates of establishment [7, 8].

This study first examines the predictive establishment methods from the available literature. As will be shown later, a number of issues arise from the lack of a common definition for establishment for both experiment and numerical simulation. We seek to develop an establishment criteria that can be used to assess establishment of both the experimental and numerical results from this study.

The establishment times that are extracted using this establishment criteria are then compared to several time normalisations which are commonly used to provide empirical guidelines to establishment times. The applicability of these methods is then assessed, and recommendations are made for their most appropriate use to help with the assessment and design of future experiments.

II. Previous Literature

A number of studies have previously examined the establishment times of separations either experimentally [1, 2, 3, 9, 10, 11], numerically [7, 8] or both [12, 13, 14, 15]. A number of different methods of assessing establishment have emerged, although very few studies even discuss their establishment criteria. Establishment criteria are in their nature often rather arbitrary and are usually tailored to the run. While no common establishment criteria exists in the literature a number of metrics for scaling/assessing establishment have emerged.

A popular method for normalising the establishment time is the 'flow time' (t_f), the time taken to travel some characteristic length by the free stream.

$$t_f = \frac{L}{U_\infty} \tag{1}$$

For experiments, L is usually model length and U_∞ is the freestream velocity. For numerical simulations, L is usually the domain length and U_∞ is usually representative of the inflow boundary velocity. This type of normalization is related to initial work done by Davies and Bernstein [4] and Gupta [5]. An experimental relationship is derived that shows the establishment times of a laminar boundary layer (t_l) over semi-infinite flat plate in a shock-tube can be expressed as:

$$t_l = 3.333\frac{L}{U_\infty} \tag{2}$$

Where L and U_∞ are the flat-plate length and the freestream velocity respectively. However, when normalizing SWBLI establishment times (t_{est}) by the flow time (t_f) there is considerable variation, from 3 t_f [13] to 150 t_f [7, 16] across various studies.

This result is perhaps not surprising, the complex flow structure resulting from a SWBLI is a long way from laminar flow over a flat plate. Large pressure gradients are present and significant mixing occurs with a large range in relevant scaling parameters. Further, the coupling between the viscous boundary-layer and the (largely) inviscid shock structure complicate matters significantly. Confusion is also created with this type of normalisation due to differences between experimental and numerical studies (this issue is discussed further in section V.A).

While the flow time is a convenient way to normalize between similar experiments it is a poor universal scaling parameter for separation establishment-times in short-duration facilities. As such, other scaling parameters have been suggested by others.

Holden [1] conducted a dedicated experimental investigation on the establishment times of the separation region generated by a compression corner. He notes that the steady state establishment time (2 ms) is approximately equal to the time taken for an acoustic wave to travel the length of the separation region (3 ms) after a steady boundary layer is established for high Mach number flows. Holden [1] suggests a time normalization based on the propagation speed of this acoustic wave, it is referred to as the 'wave time' (t_w) and is given as:

$$t_w = \frac{L_{sep}}{\bar{a}_\delta} \tag{3}$$

Where L_{sep} is the separation length and $\bar{a}_\delta$ is the average speed of sound through the boundary layer which can either be directly calculated if information is available or evaluated from the average boundary-layer temperature ($\bar{T}_\delta$) using:

$$\bar{a}_\delta = (\gamma R \bar{T}_\delta)^{0.5} \tag{4}$$

Where ($\bar{T}_\delta$) can be calculated using the Eckert reference temperature:

$$\bar{T}_\delta = 0.5(T_w + T_\infty) + 0.11 Pr^{0.5}(\gamma - 1) M_\infty^2 T_\infty \tag{5}$$

Here the wave-time normalization is very similar to the flow time, except it uses physical quantities locally at the separation in order to normalize, which is likely to be more appropriate given that shock-wave induced boundary-layer separation is known to be more sensitive to local conditions at separation than those of the freestream [17, 18]. Although, it should be noted that large differences in the establishment time of the boundary-layer can occur for different experiments, for example sharp verses blunt nosed bodies. As the SWBLI relies on the boundary-layer conditions, experiments are unlikely to scale well with local conditions if the boundary-layer establishment times vary significantly.

Ihrig et al.[3], had previously performed an analytical evaluation where they consider the time scales for phenomena they believe important to the establishment of a generic separation. They consider three important time scales: acoustic-wave time (t_w, as defined above), mass-transfer time (t_m) and heat-transfer time (t_H):

$$t_w = \frac{L_{sep}}{\bar{a}_\delta} \tag{6}$$

$$t_m = \frac{L_{sep}}{U_e \Gamma} \tag{7}$$

$$t_H = \frac{L_{sep}}{U_e S t} \tag{8}$$

Where L_{sep} is the separation length, U_e is the boundary-layer edge velocity, Γ is a mass mixing parameter and St is the Stanton number.

Ihrig et al.[3], note that the wave time is the quickest time scale, with the heat transfer time taking the longest. The ratio of the two quantities hints at possible differences in convergence time scales of the two quantities:

$$\frac{t_H}{t_w} = \frac{1}{M_e S t} \tag{9}$$

Assuming typical Stanton numbers for a turbulent flow in a supersonic intermittent facility, St= 0.01 [2, 3, 10], it is possible estimate the ratio of heat transfer times to wave times:

$$\frac{t_H}{t_w} = \frac{100}{M_e} \tag{10}$$

Holden [1], performed a number of experiments over a wide range of local Mach numbers. Figure 1 shows establishment times for the wall pressure normalised by the analytical wave time (equation 6). Holden [1] claims that for high Mach numbers (12-20) the establishment times of surface pressure and heat transfer become similar; a claim which is supported by equation 10. Although, as shown later, this assumption does not appear to be true for all experiments assessed in this study.

As seen in figure 1 the wave time seems to provide a robust normalisation for the cases it considers, providing good and relatively accurate estimates of the establishment times for these cases. Of all the normalisations inspected, the heat transfer and wave times appear to provide the most promise of providing a universal scaling parameter. Both quantities use local conditions close to the interaction which is not only physically better in terms of the quantities thought to drive the interaction but also helps to account for different model geometries etc.

More recently Mallinson et al.[6] conducted a dedicated study where they examine establishment times from their own data on a compression corner and that of others [1, 2, 12], as shown in figure 2. Here a normalization is employed that uses total enthalpy (h_0) to expresses establishment times in terms of 'flow lengths':

$$l_f = t_{est}(2h_0)^{0.5} \tag{11}$$

As seen in figure 2, this type of scaling parameter works relatively well in reducing the establishment times in three of the facilities examined. This method of normalisation will be examined further in this study. Although, as will be shown later (Section V.C) this type of normalisation is actually very similar to the flow length and hence it is likely to suffer from the same drawbacks.

III. Present Study

This study presents results from both experiments and numerical simulations that were conducted to examine the interaction between a laminar boundary layer and a flare induced separation region on a blunt-nosed cylinder.

A series of experiments and numerical simulations were used to design a SWBLI such that it was separated for a laminar boundary-layer and collapsed for a turbulent one. Experiments show that the separation is very sensitive to the conditions of the boundary layer [15, 19, 20], so much so that the boundary-layer state (laminar/transitional/turbulent) can be inferred from the SWBLI shock-structure (separated/collapsed). All cases considered in this study examine the laminar boundary layer case.

When designing the test article, great care was taken to ensure establishment of the SWBLI by combining results

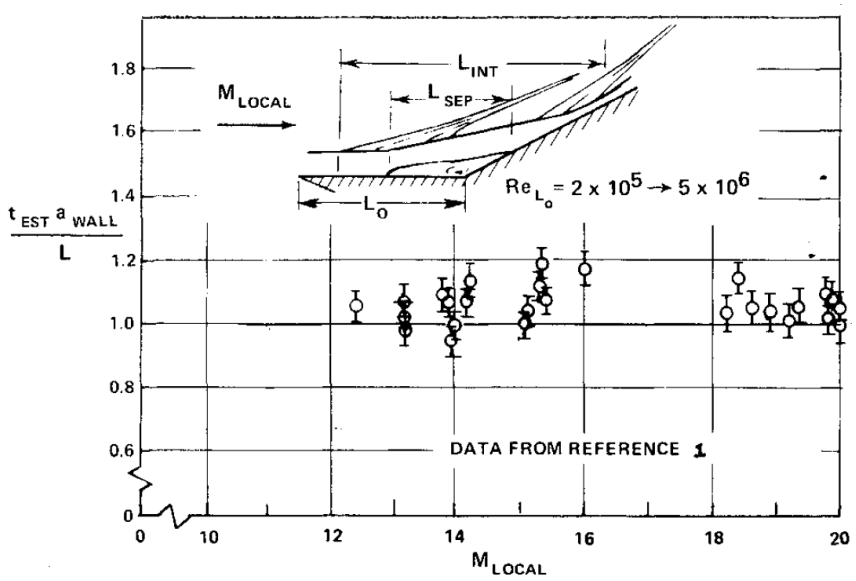

Figure 1: Experimental surface pressure establishment time normalised by the wave-time (t_w). Figure from Holden et al. [1].

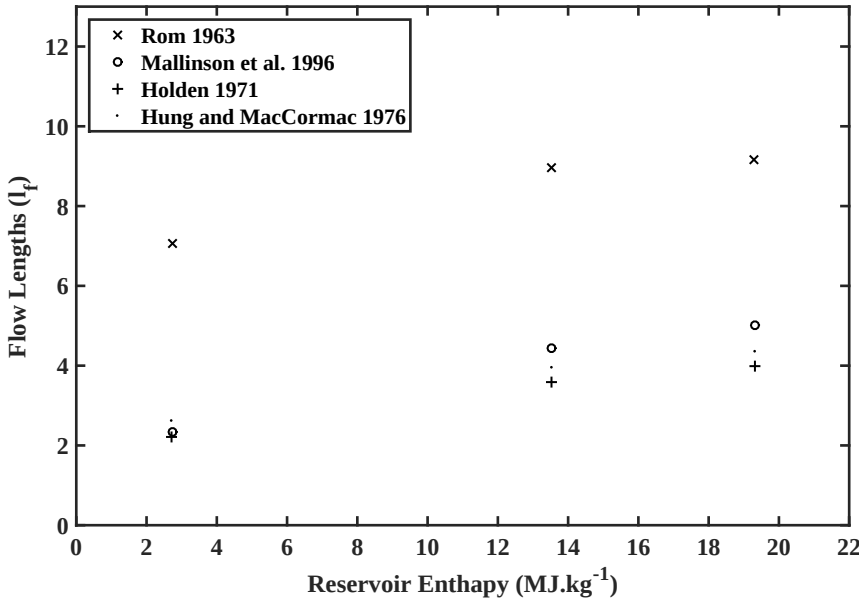

Figure 2: Establishment time normalisation using 'flow lengths' reproduced from data in Mallinson et al.[6].

from preliminary experimental and numerical results. This section examines that process of assessing establishment. Being a joint experimental/numerical study facilitates direct comparison between both experimental and numerical establishment times for identical cases. In this sense, this study serves as a benchmark study for assessing establishment times.

A. Facility

Experiments are conducted in The Imperial College Number 2 Gun Tunnel: a Mach 8.9 free piston facility. A detailed study of the tunnel conditions has been previously conducted by [21], an overview is given here. The test gas is nitrogen which reaches a nominal unit Reynolds number of 47x10^6 m^{-1}. The facility is intermittent, it is considered established after 10 ms and the steady-run window lasts 6 ms. It is important to note that establishment of the facility should not be confused with establishment time of the SWBLI. When the test–flow is steady, a highly axisymmetric 1.8m test diamond is formed from a 0.35 m diameter nozzle. Test conditions are given as:

P_∞ = 3kPa	T_∞ = 68 K	Unit $Re_\infty = 47x10^6$ m^{-1}
$U_\infty = 1491 ms^{-1}$	M_∞ = 8.91	$h_\infty = 1.2 MJkg^{-1}$

Table 1: Tunnel freestream conditions as measured by Mallinson et al. [21].

$\delta_{99} = 1.7mm$	P_e = 4.6 kPa	T_e = 339 K	Unit $Re_e = 3.01x10^6$ m^{-1}
	U_e = 1283 ms^{-1}	M_e = 3.44	L_{sep} = 0.023 m

Table 2: Boundary-layer edge conditions just upstream of the interaction region. Conditions taken from numerical simulation. Boundary-layer edge based on 99% thermal boundary-layer.

The model used for this study is a blunt nosed axisymmetric cylinder fitted with an eight degree flare at x=0.212 m from the nose, as shown in figure 3. A separation bubble forms at the cylinder-flare junction. The blunt nose of the model (figure 3b) leads to a large entropy gradient through the flow field. Conditions close to the wall are very different from those of the outboard flow. Local boundary layer edge conditions just upstream of the interaction are given in table 2.

B. Surface Pressure, Heat-Transfer and Schlieren Measurements

Experimental surface quantities through the interaction region are measured using thin-film heat-transfer gauges (Schultz and Jones [22]) or surface mounted piezo-resistive pressure sensors (Kulites). Synchronised schlieren video was also used to further diagnose the shock structure away from the wall.

As seen in figure 3 (a), two sensor modules are used for each run. One module is mounted flush to the body, upstream of the 'cylinder-flare junction': the location where the blunt-body ends and the flare begins (x=0.212 m). The second sensor module is mounted flush to the flare, downstream of the cylinder-flare junction. The separation region straddles the cylinder-flare junction and the sensor modules span the entire interaction region and a small

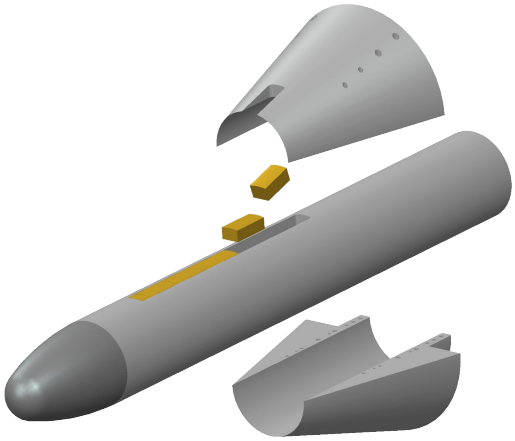

(a)

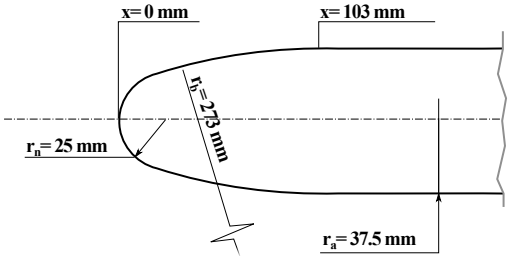

(b)

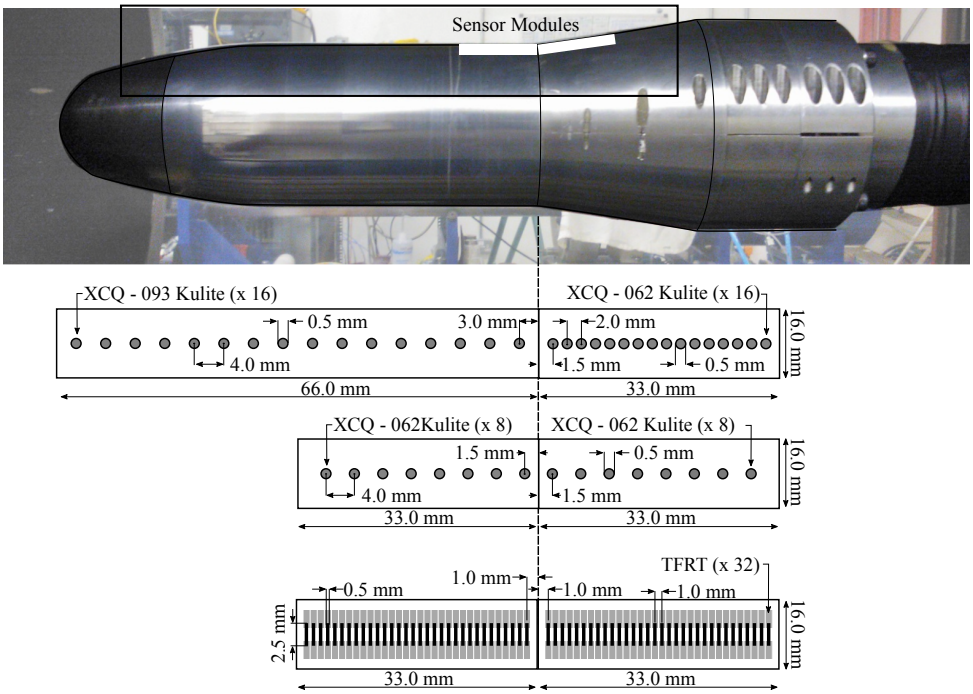

(c)

Figure 3: Model Geometry. (a) Exploded diagram showing blunt-nosed centre body, modular sensor inserts and the flare. (b) Nose section with dimensions. (c) Picture of model assembly with sensor module locations overlaid and sensor configurations shown below (not to scale). Black box marks field of view in figure 8.

region up- and downstream of it.

Data is acquired over a maximum of 64 channels at 100 kHz and lowpass filtered at 50 kHz using an analogue filter. Each channel is linked to a Flyde (FE-759- TA) card, which provides high fidelity gain and offset options to the incoming signal. Four HGL Dragonfly (DF24F) analogue to digital converters digitise the signal across 16 cards each and feed this information to a PC for storage. Signal to noise ratio for the analogue to digital converters is 120 dB [23].

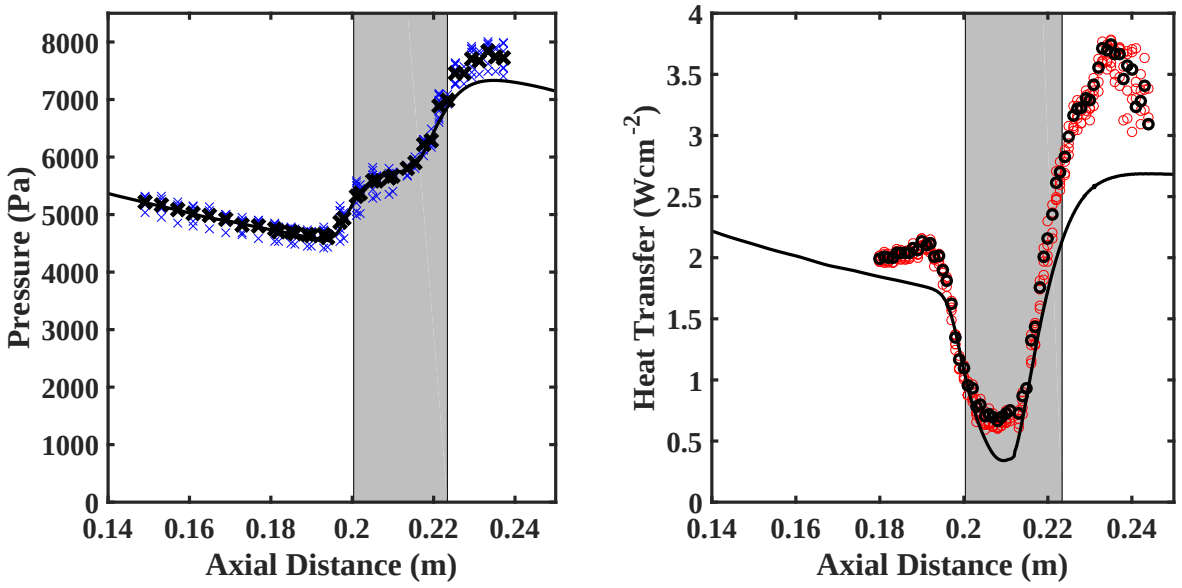

(a) (b)

Figure 4: Experimental ensemble averaged steady-state (markers) and numerical (solid line) results for surface pressure (a, crosses) and heat transfer (b, circles) through the interaction region. Coloured markers show individual run averages, black markers show average for whole data set. Separation region, extracted from CFD, is shown shaded in gray.

The pressure modules featured Kulites that were mounted below the surface, inside a small cavity connected to the surface by a 0.5 mm diameter tapping in order to give better spacial resolution. Two different surface pressure sensor modules were used as detailed in figure 3(c). The run averaged, steady-state laminar surface-pressure distribution for 10 different experimental runs is shown in figure 4(a) with comparison to the predicted numerical distribution. Error in measuring surface pressure is assessed as 2% [15].

The thin-film heat-transfer gauges use a thin platinum film that is painted onto a ceramic MACOR substrate, it has the same streamwise spacial resolution as the surface pressure measurements (0.5 mm). The resistance of the strip is measured and heat transfer can be inferred [22]. A single sensor configuration is used as shown in figure 3(c). The run averaged, steady-state laminar heat-transfer rate is shown in figure 4(b) with comparison to the numerical prediction. Error in measuring heat-transfer is assessed as 10%.

The schlieren images are acquired using a Phantom v5.2 or Photron Fastcam SA1.1, at a maximum frame rate of

100,000 images a second. All images are taken with a horizontal knife edge. Exposure times are 0.01 ms.

C. Mesh and Time Convergence of the Numerical Simulation

The numerical scheme used for this study has been described previously [24] and only an overview is provided here. The scheme is time accurate, it splits the Navier-Stokes convective/diffusive terms and where appropriate these terms are decoupled in space. Different schemes are used to solve each of these terms using an appropriate sub-time step. The solution at each time step is then assembled from the summation of each of the solutions from the sub-time steps.

The 2D Euler equations are decoupled using a second order splitting method [25]. An up-wind second order Godunov solver is used to solve each 1D Euler equation [26]. The viscous terms of the Navier-Stokes diffusion equations are solved explicitly using a two step Runge-Kutta method. This numerical solver does not model non-equilibrium effects from the dissociation of N_2 as the flow is considered 'cold' and does not significantly dissociate.

Figure 4 shows the ensemble averaged (for each data set), steady-state experimental and time-converged numerical results for surface pressure (a) and heat transfer (b). Agreement between experimental and numerical surface pressures is very good for the entirety of the incoming boundary layer and the separation region. However, after reattachment an increasing disparity is observed. It is believed that the discrepency at reattachment is due to the presence of 3D effects which the solver can not capture. Surface oil-flow visualisation (not shown) revealed the presence of streamwise vortical 3D structures which resembled Görtler vortices.

The numerical simulations are impulsively started and were performed on the entire body. The mesh is shown in figure 5, it is curvilinear and is locally fitted to the bow shock and the boundary-layer at the body surface to allow better resolution of both. The mesh also contains a high degree of node optimization, with nodes clustered in areas of high gradient such as the boundary-layer, nose and separation regions.

The numerical simulations are grid converged such that doubling of the grid resolution results in less than a 1% change in the length of the separation bubble. The separation length is chosen as the metric of grid convergence here as it requires good resolution of the free shear layer, local shock structure and boundary-layer in the local interaction region.

Figure 6 shows history profiles for heat-transfer at 21 evenly spaced locations along the surface of the separation region. These history profiles are used to asses the time convergence of the numerical simulations. The authors wish to stress that it is important to note that the time convergence and establishment time of the numerical simulation are not equivalent.

Time convergence is a purely numerical metric, it represents some measure of the ability of the simulation to converge to a steady solution relative to the machine accuracy of the computer. Establishment time is classically an experimental quantity, it is a measure of the time taken for the time-averaged flow structure to establish, usually to within measurement error. As experimental accuracy (typically 1-10%) is much larger than machine accuracy (2^{-53} for double precision), time convergence is a much stricter criteria than establishment. This point is very relevant to

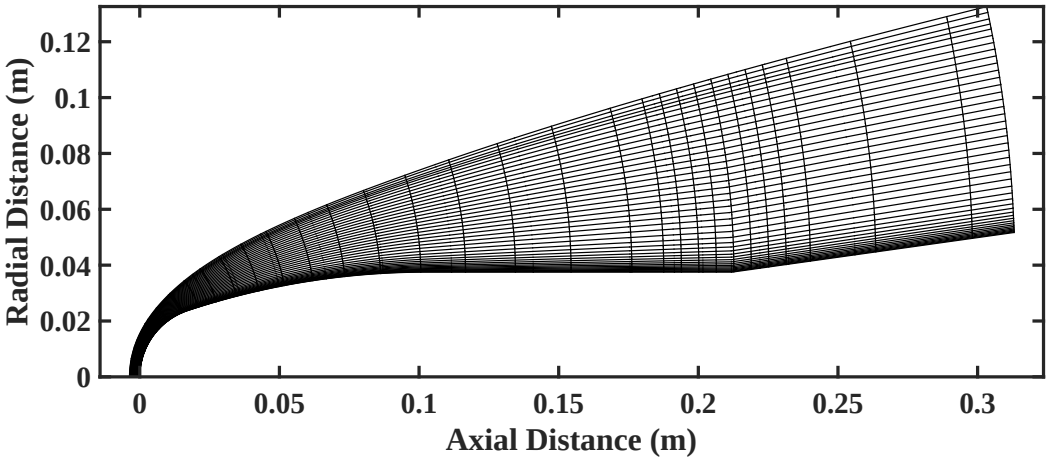

Figure 5: Converged CFD mesh used for the blunt-nosed body. Only every 30th mesh node is shown.

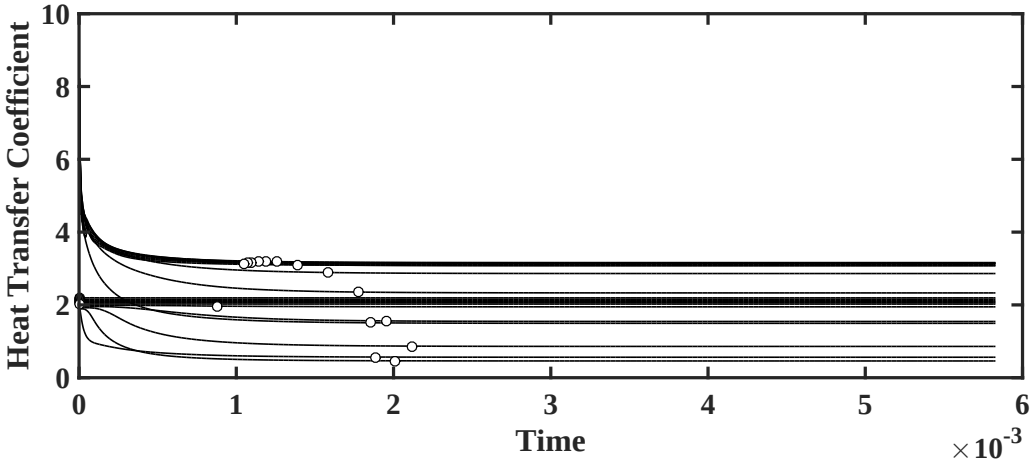

Figure 6: Numerical 99% convergence plot times (circles) at various stations for heat transfer coefficient histories (solid lines).

later discussion (section V).

As shown in figure 6, time convergence of the separation is asymptotic and so technically never truly converges in any reasonable amount of time even to within machine accuracy of the solution. A visual inspection of the quantities in figure 6 clearly shows their convergence, with the traces remaining unchanged after t≈2 ms and the simulation being run for another t≈4 ms. However, some convergence criteria should be selected.

For this study a numerical solution was considered time converged when the amount of time taken for the solution to reach 99% of the final history values at all stations through the interaction occupied less that 50% of the total time that had passed in the solver (figure 6). In other words, the simulation was run for atleast twice the time taken for the simulation to reach 99% of the final value. This ensures the simulation is far into asymptotic convergence, well past 99% converged. This criteria is much stricter than the establishment criteria that is applied to the numerical simulation later. Hence, relative to the analysis that will be performed the numerical solutions can be considered time converged.

D. Experimental Steady-Run Conditions

All of the establishment metrics discussed in this study come from different tunnels and model geometries. Most of the metrics rely on the concept of being able to scale establishment times based on some pertinent flow quantity(ies) for similar models in similar facilities. This results in a number of different scaling parameters which are appropriate for different 'families' of facilities/experiments. While this approach is reasonable for local comparisons it makes it difficult to assess global trends as free-stream establishment times in different experimental facilities can vary significantly. For example: free-piton shock-tunnels establish very quickly as stagnation conditions are achieved after a single reflected shock at the nozzle throat [27]. This renders the starting process relatively quick and the process of the tunnel start and model start can be delineated [28]. This facility is a gun-tunnel, stagnation conditions are achieved through multiple reflected compression shocks which ramp-up the tunnel to steady-run conditions over a much longer period [21]. The entire experiment inside a free-piston shock-tunnel can finish before a gun-tunnel facility is steady and hence direct comparison of experiment starting times is clearly not possible. Further, many numerical studies are started either impulsively or from some previous solution. This even makes direct comparison between experimental and numerical starting times of the same experiment difficult, as no common reference point exists from which to examine establishment of the SWBLI.

This problem is further exacerbated by geometry related problems, as each particular model geometry will also have some model establishment time, the time taken for the flow local flow features to establish in a steady flow. An illustrative example of how the model establishment time can vary in the same facility is given below: The vehicle for this study is a blunt nosed cylinder that generates a laminar boundary-layer. This results in very low velocities at the nose, which take a considerable amount of time to establish. When comparing the establishment time of the inflowing boundary-layer at the interaction location between a blunt-nosed cylinder and a sharp plate with the same characteristic length in the same flow, very different times will be observed.

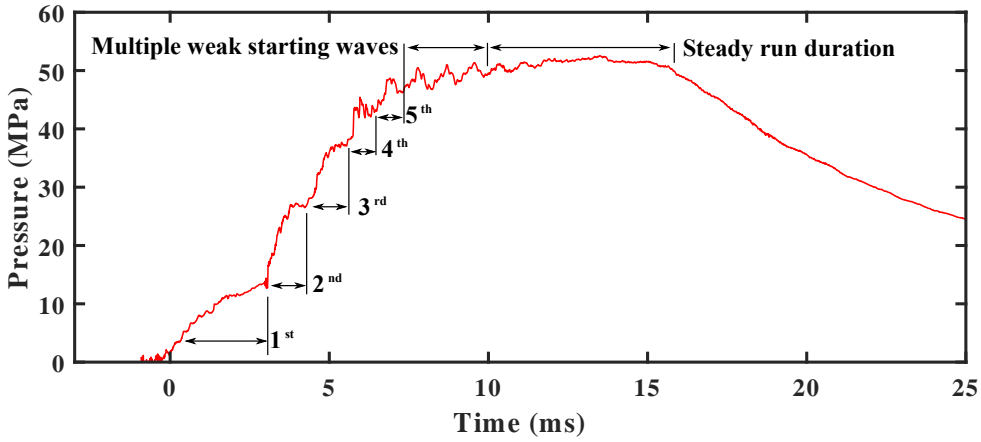

Figure 7: Time history of the nozzle-throat pressure-transducer.

In order to achieve meaningful comparison between different cases it is very important that establishment of the SWBLI is considered relative to some feature in the flow which is as universal as possible. The most appropriate time to compare between cases is likely the establishment of the boundary-layer flow. However, the establishment of the gun-tunnel is complex and understanding the starting time of the free-stream is not trivial. Hence, we wish to examine the starting process in depth.

A gun-tunnel facility is an intermittent facility which operates on the concept of building a high enthalpy reservoir at the nozzle throat. This is achieved through multiple compression waves, which bounce between the piston-head and the nozzle throat. This results in the gun-tunnel ramping up through a complex series of nozzle/model starts with diminishing strength that asymptotically approach the steady-run conditions. This process is illustrated in Figure 7, which shows the time histories for the nozzle-throat pressure-transducer, a number of the starting waves are indicated on the figure. The establishment of the SWBLI generated by the model is intimately linked to the establishment of the flow around the model which is in turn dependent on the freestream. Many of the starting waves have a strong effect on the structure of the flow field, often distorting the bow shock or collapsing the separation region. The following discussion examines the starting process of the model flow field more closely.

Figure 8a shows the time histories during the starting process for the nozzle-throat pressure-transducer and the transducer immediately downstream (x= 0.2135 m) of the cylinder-flare junction (post-junction pressure transducer). Figure 8b shows the post-junction (x= 0.2135 m) heat-transfer rates. Various times of interest are marked in these two figures and wide-field schlieren images for those times are shown in figure 8c-n which relate to the conditions before, during or after large perturbations to pressure or heat-transfer.

Owing to the faint nature of the axisymmetric shock-system it can be difficult to see details of the flowfield in the images such as the separated shock-structure or the boundary-layer. As such the separated SWBLI does not appear present (for example figure 8i). However, the collapsed (attached) SWBLI is visible owing to the stronger shock

configuration and can be seen clearly (for example figure 8j). With the exception of figures 8c-d, which are associated with the first starting shock, all of the schlieren images which do not show a single attached shock at the cylinder-flare junction should be considered separated. The reader is reminded that the SWBLI was selected to be separated for a laminar flow and collapsed for a turbulent one. Hence, strong disturbances to the boundary-layer can be inferred from the collapse of the SWBLI to the stronger attached configuration.

The boundary-layer on the model likely establishes relatively quickly after the first starting-shock, as evidence by the separated SWBLI in figure 8f (which has not been influenced by the second starting-shock yet). However, the three strong starting-waves that follow (figures 8f, k and h) distort the bow-shock and boundary-layer significantly, which results in the collapse of the SWBLI in figures 8g, j and l. It is clear that neither the boundary-layer nor SWBLI could be considered established before the last strong starting shock (t=6.51 ms). Some short-time after the last strong shock the boundary-layer likely establishes. Hence, t=6.51 ms is used as an estimate of the boundary-layer establishment, this value agrees well with later analysis of the boundary-layer establishment (section IV.B).

IV. Establishment of the Shock-Wave Boundary-Layer Interaction

A range of different establishment times have been proposed and observed in the literature and it is difficult to isolate the most relevant one. Part of the problem comes from a lack of any common agreement on an establishment criteria. This section seeks to develop an establishment criteria that can be applied to both experiment and simulation. These establishment times can then be compared with the wider literature in section V.

A. Establishment Criteria

Any establishment time is intended to represent the time taken for some time varying quantity ($Q(t)$) to converge to, and remain within some arbitrary acceptable threshold of the steady-state value ($Q_{ss}(t)$). Here, the steady-state value $Q_{ss}(t)$ is shown as a function of time (t) as many experimental facilities still vary (are not statistically stationary) through regions usually considered steady, which is relevant later. The establishment criteria can be expressed as:

$$(1 - A)Q_{ss}(t) < Q(t) < (1 + A)Q_{ss}(t) \tag{12}$$

Where A is some appropriate fraction of the steady-state value. However, this criteria is not very robust, as $Q(t)$ usually contains variation caused by some combination of unsteadiness, noise, measurement error, machine error, etc. If this variation is significant in relation to establishment, then the establishment criteria described in equation 12 breaks down.

Some variation occurs at frequencies above those that are likely to be associated with establishment and as such it can be ignored. Hence, the signal can be low-pass filtered and the establishment criteria becomes:

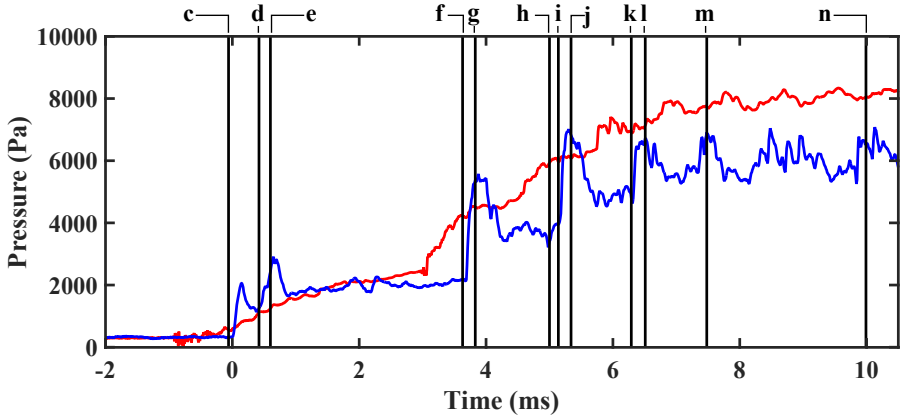

(a) Pressure histories.

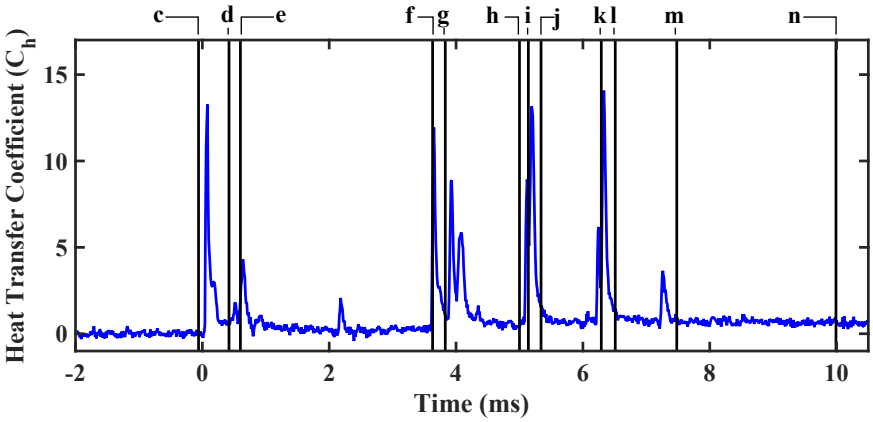

(b) Heat transfer history.

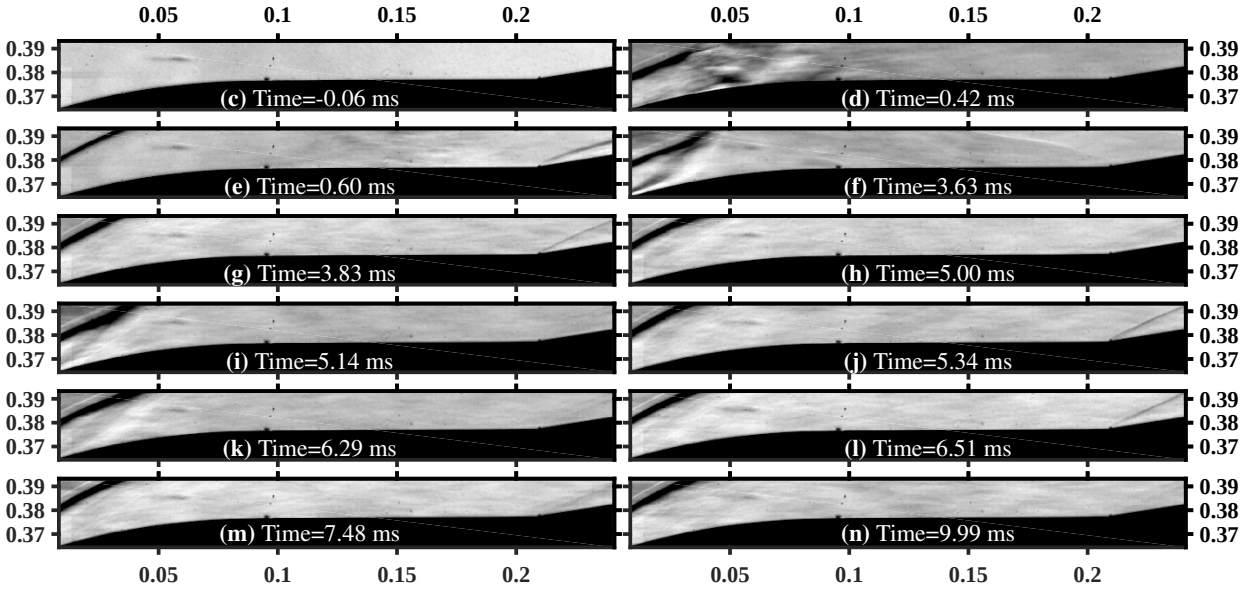

Figure 8: Starting process for test facility. (a) Pressure history at x=0.2135 m (blue) and the nozzle throat (red). Throat history is arbitrarily scaled for comparison. (b) Heat-transfer history at x=0.2135 m. (c) - (n) Schlieren photographs (100,000 fps) of the model at times marked in (a) and (b). Time is offset such that zero coincides with the tunnel start time. Field of view from schlieren is shown in figure 3.

$$(1 - A)\hat{Q}_{ss}(t) < \hat{Q}(t) < (1 + A)\hat{Q}_{ss}(t) \tag{13}$$

Where $\hat{Q}$ denotes the signal that has been low pass filtered. $\hat{Q}_{ss}(t)$ can be further expanded to express it in terms of a true time-invariant component ($\bar{Q}_{ss}$) and some time-varying deviation from this value which has also been low-pass filtered ($\hat{Q}_{Var}(t)$):

$$\hat{Q}(t)_{ss} = \bar{Q}_{ss} + \hat{Q}_{Var}(t) \tag{14}$$

Approximations for both $\bar{Q}_{ss}$ and $\hat{Q}_{Var}(t)$ are sought as they are unknown. $\bar{Q}_{ss}$ is approximated as the steady-state value achieved from experiment/simulation. If $\hat{Q}_{Var}(t)$ is assumed to have a normal distribution then its range over the steady-state window can be expressed as some multiple (n) of the standard deviation of the steady-state signal σ_{ss}:

$$\hat{Q}(t)_{ss} \approx \bar{Q}_{ss} \pm n\sigma_{ss} \tag{15}$$

The chance that the actual time varying, lowpass filtered signal $\hat{Q}(t)_{ss}$ is contained within the bounds set by $\bar{Q}_{ss} \pm n\sigma_{ss}$ is essentially driven by the choice of n. Substituting equation 15 into the convergence criteria from equation 14 gives:

$$(1 - A)(\bar{Q}_{ss} \pm n\sigma_{ss}) < \hat{Q}(t) < (1 + A)(\bar{Q}_{ss} \pm n\sigma_{ss}) \tag{16}$$

Equation 16 represent the general form of the establishment criteria developed for this study. However, this criteria relies on appropriate choice of values for A, n and the cut-off frequency for low pass filtering. It is important to stress that the most appropriate values for each of these quantities could change significantly between facilities.

The term $(1 \pm A)$ represents the degree of arbitrary convergence to the 'true' steady-state value, the choice of A drives this convergence. For this study, experimental accuracy for surface pressure and heat-transfer is approximately 1-10%. Given experimental quantities are used to validate numerical simulations it seems reasonable to consider both converged when they converge to within experimental accuracy, taken here at the upper limit of 10%: hence A is approximated as 0.1.

The term $(\bar{Q}_{ss} \pm n\sigma_{ss})$ essentially compensates for variation in the average quantity of interest, the choice of n is analogous to setting the confidence interval. For this study the value of n is chosen as 1, meaning that (assuming a normal distribution) approximately 70% of the steady-state signal variation as being within variation associated with establishment.

The choice of cut-off frequency essentially sets some limit on the time-scales that are assumed to effect the establishment to a steady-state. As identified previously, it is likely that there is some characteristic time-scale associated with convective and diffusive time scales in the interaction. Of these time-scales the diffusive is limiting. For this

study the order of the heat-transfer time (equation 8) is used as an approximation of diffusive times-scales, which is of the order 1 ms and so frequencies above 1 kHz have been removed.

Hence, the specific convergence criteria for this study is:

$$0.9(\bar{Q}_{ss} - \sigma_{ss}) < \hat{Q}(t)_{1kHz} < 1.1(\bar{Q}_{ss} + \sigma_{ss}) \tag{17}$$

Obviously, this criteria is sensitive to the selected magnitude of experimental error, the weighting placed on the standard deviation of the signal and the time-scale chosen to filter the signal at. Choosing different values results in different establishment-times. Given the great variation between facilities it is very likely that other studies would chose very different quantities. However, the order of magnitude of the establishment times in this study remains the same for a relatively wide choice of these values. Given the wide range of establishment times reported in the literature, especially when comparing experimental and numerical results, this criteria is a significant improvement.

B. Experimental Surface Pressure and Heat-Transfer Establishment Times

The laminar data set consists of 10 surface pressure and 6 heat-transfer runs. High-speed experiments are difficult and most studies rely on measurements from a only single run for each case examined. Hence, while the averages examined here are unlikely to be statistically converged they represent cases that are considerably more converged than much of the literature.

The establishment criteria from equation 17 was applied to the surface pressure and heat transfer runs and ensemble averaged for each data sets. Figure 9 shows that the surface pressure and heat-transfer measurements upstream of the region of influence of the interaction ($x < 0.19$ m) establish at a relatively uniform time: 6.3 ms and 6.5 ms respectively. This value compares well with the time extracted from the analysis of the tunnel establishment process (6.5 ms) discussed in section III.D.

Figure 9 shows considerable range is observed in the surface-pressure establishment times through the interaction, where as the heat-transfer interaction region establishment times show a tighter distribution with less variation. The establishment time for the separation region is taken as the average establishment time through the region, 6.5 ms for surface pressure and 8.6 ms for the heat-transfer (figure 9).

These establishment times are still specific to this facility. Several common points of reference have been identified in order to try and separate establishment of the SWBLI from establishment of the facility. Previous assessment of the interaction implied that the last strong starting wave was an appropriate time (6.5 ms). Assessment of incoming boundary-layer for both surface quantities provides estimates of the boundary-layer establishment time that are in good agreement with this value. Hence, establishment of each quantity is given relative to its specific boundary-layer establishment time. This is a similar approach to that employed by [13]. Subtracting the surface pressure and heat-transfer boundary-layer establishment times gives the surface-pressure establishment time as 0.2 ms and the heat-

transfer establishment time as 2.1 ms.

C. Numerical Surface Pressure and Heat-Transfer Establishment Times

The first numerical simulations for this study were first performed on an unflared blunt-nosed cylinder in order to get a solution for the boundary layer. A new mesh was generated with a flare and started from the solution with a converged boundary-layer. The mesh was then iteratively refined until the separation length changed by less than 1%. All of the steady-state CFD results use data from the mesh converged run. However, the cost of the mesh converged simulation was high and each refined mesh was started from the converged solution of the last. It was not feasible to start the simulation from the converged boundary-layer solution or simulate the tunnel starting conditions.

In order to investigate establishment times we were forced to use a lower resolution mesh which could be started from the converged boundary-layer solution and run continuously to convergence of the steady-state. The resolution used shows a 10% change in the separation length compared to the mesh converged solution. It is noted that anticipated experimental error is of the order 10% and in this sense the degree of error introduced this way is still approximately equal to experimental error.

Obviously, basing establishment times on a mesh that is not converged is questionable, however other studies will face similar challenges when attempting to use numerical estimates of establishment. Part of this investigation is concerned with assessing current CFD capabilities when estimating establishment times.

The establishment criteria from equation 16 was applied to the numerical surface pressure and heat transfer time histories. Establishment times at various locations through the interaction region for both the pressure and heat transfer times are shown in figure 10.

Some of the trends seen in figure 9 are also observed in figure 10, especially the peak at separation. The average establishment time for pressure and heat-transfer through the interaction region is 0.111 ms and 0.771 ms respectively. These readings are already given relative to an established boundary-layer, as the simulation starts from the converged boundary-layer solution.

In addition to the eight degree flare case that was experimentally investigated a number of other flare-angle cases were also simulated. Given that the eight degree flare simulation gives reasonable estimates of the establishment times, the other flare angles will also be considered for this study as they provide data for the case where flow conditions are held constant and model geometry is changed. Using the same convergence criteria as for the eight degree flare case the heat transfer and wave times for the various flare angles are shown in figure 11. The heat transfer and wave times represent the time taken for the heat transfer and surface pressure through the interaction to establish in an established flow.

Figure 12 shows the numerically predicted separation length for all of the cases. While discussed in more detail later, it is important to note that the establishment times seem to show a non-linear trend while the separation length is approximately linear. For the same flow conditions the separation length and establishment times do not scale

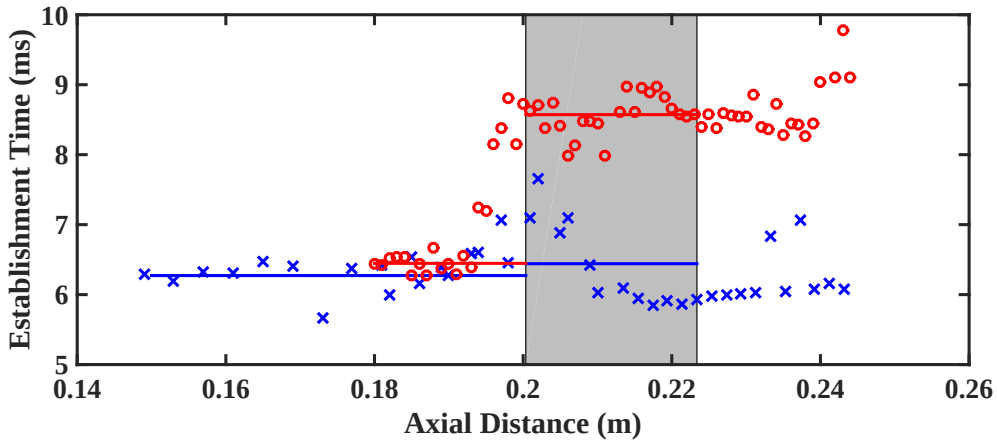

Figure 9: Run-averaged establishment times for surface-pressure (blue) and heat-transfer (red). Grey region shows separation region. Flat lines mark average times for their respective regions.

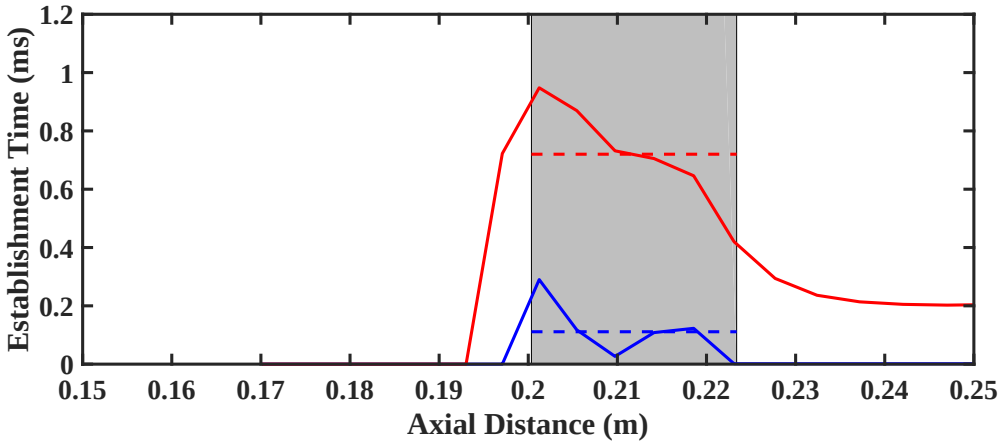

Figure 10: Numerical establishment times for surface pressure (blue) and heat-transfer (red) started from a converged boundary-layer solution. Grey region shows separation region. Flat dashed lines mark average times through the separation region.

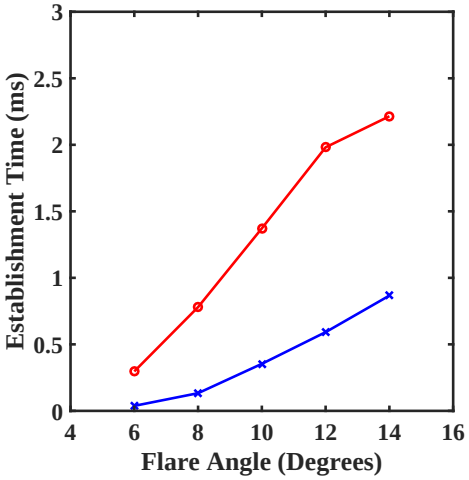

Figure 11: Numerical surface-pressure (blue) and heat-transfer (red) establishment times for various flare angles.

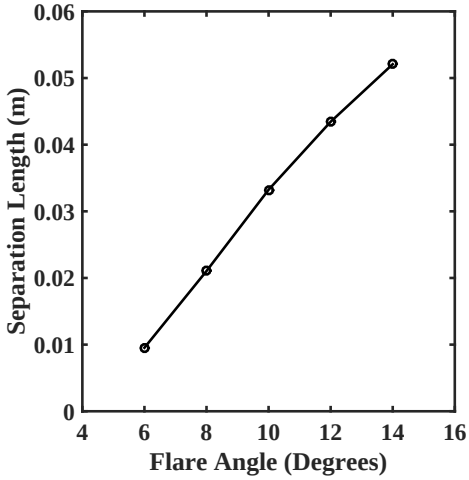

Figure 12: Numerical separation lengths for the same flow conditions with changing flare angle.

linearly with each other. As will be discussed later, this causes issues for all of the establishment scaling parameters investigated in this study.

V. Discussion

Experimental and numerical establishment times for the eight degree flare are shown in figure 13, with average values shown in Table 3. Agreement is reasonable, although the numerical simulations seem to under predict establishment times by a factor of $\approx$ 2. Particular disparity is seen at separation, which is very sensitive to disturbances in the incoming boundary-layer. One possible reason for the difference is due to the starting process of the tunnel. In the experiment, after the boundary-layer is established, weak starting-waves that continue to wash through the test section and perturb the interaction, delaying the time taken to reach establishment. In contrast, the numerical simulation is started impulsively with constant inflow conditions from a converged boundary-layer solution.

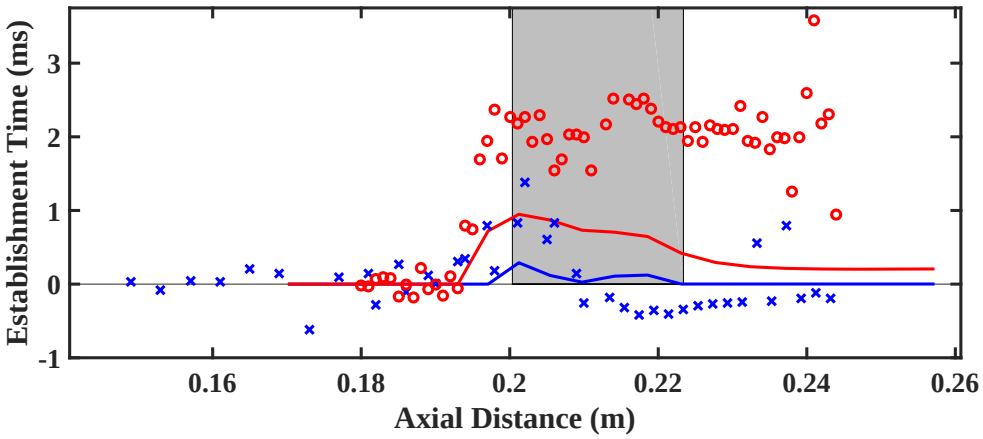

Figure 13: Experimental (markers) and numerical (solid) establishment times for surface pressure (blue) and heat-transfer (red) relative to the boundary-layer establishment. Grey region shows separation region.

	Surface Pressure (ms)	Heat Transfer (ms)
Experimental	0.2	2.1
Numerical	0.111	0.771
Factor	1.8	2.7

Table 3: Experimental and numerical establishment times for the eight degree flare.

It is now possible to assess the establishment times of this facility within the context of the various metrics often employed from the wider literature. As discussed previously (section II), a number of methods have emerged as promising candidates for estimating/normalising establishment times between facilities. These are: Numerical Simulation, the Wave and Heat-Transfer Times and the Flow Length.

A. Numerical Establishment Times

Numerical simulation is the most promising tool for predicting establishment times. Given adequate knowledge of boundary conditions, sufficient schemes, mesh resolution and computational time, the numerical simulation should provide accurate results. However, at such high Reynolds numbers, with limited experimental data this can be very difficult to achieve and so approximations and compromises must be made. Given the current state of numerical simulations, how accurate can their predictions be considered?

As shown in section V, the experimental and numerical establishment times assessed for this study are a factor of two apart. Swantek et al.[11] notes that numerical establishment times are often significantly longer than those seen in experiments. It is difficult to assess possible reasons for this discrepancy, in part due to a lack of available data. However, a significant portion of this disparity likely originates from the direct comparison of the quantities that experimental/numerical studies tend to consider for establishment.

A minor problem arises due to the quantities that experimental and numerical solutions use for normalisation. A quantity typically chosen in numerical studies is the characteristic time:

$$t_c = \frac{L_{dom}}{U_{inflow}} \tag{18}$$

Where L_{dom} is the domain length and U_{inflow} is usually some characteristic boundary inflow velocity.

The characteristic time is a quantity which is analogous to the flow time (equation 1) and the temptation is to compare these quantities. However, the domain length is often much smaller than the model length due to high free stream Reynolds (usually the result of high velocities) and hence the characteristic time is often a smaller normalising quantity than those used by experiments.

The largest problem however, arises from the fundamental choice of 'establishment criteria' typically chosen by experimental/numerical studies. For example: several recent studies numerically simulated the flow over the entire model for a double angle cone [7, 8, 16]. Here, all three studies find similar establishment times of 100-150 t_c. For these three cases the domain length was the model length and U_{inflow} was taken as the freestream conditions and hence the characteristic time becomes the flow time. A recent experimental study [11] of a very similar double angle cone experiment suggest that experimental establishment times are of the order $1t_f$. In this case the establishment times have been normalised by the same quantity and yet show a difference of two orders of magnitude. This difference is far too large to be accountable to differences between the relatively similar experiments.

The reason for such a large difference is due to the choice of the actual 'establishment time'. As previously discussed (section III.C) numerical simulations are concerned with convergence time: the time taken for the simulation to converge relative to machine accuracy. Experimental studies are concerned with the establishment time: the time taken to converge to the steady-state value relative to measurement error. These quantities are very different.

Examining the studies of [7, 8, 16] it is apparent that they state a convergence time. Time convergence of the

separation region is asymptotic and so this metric produces large times ($\approx 150t_c$). Compared to experiments, where error is atleast a few percent and robust assessment of establishment is difficult, this type of convergence criteria is extremely strict. For this reason, it is not possible to meaningfully compare the convergence time of a numerical simulation to the establishment time of an experiment.

It is important to stress that this finding is not a criticism of any of the studies mentioned above. The difference is purely an artefact of experimental and numerical studies being concerned with different time quantities. This problem is the reason a reason that a common establishment criteria was developed for this study (section IV.B). If this criteria was applied across both the experimental [11] and numerical studies [7, 8, 16] mentioned here then it is very likely much better agreement would be observed.

B. Heat Transfer and Wave Times

The heat-transfer and wave times of an interaction represent some characteristic time scale associated with the interaction. If physically meaningful, then it should be possible to normalise across some range of different experiments with the aim of extracting trends that allow prediction of establishment times for future experiments.

Using the equations from [3] it is possible to calculate analytical estimates for both the wave time (t_w) and heat transfer time (t_H) for this study:

$$t_w = \frac{L_{sep}}{\bar{a}_\delta} \tag{19}$$

$$t_H = \frac{L_{sep}}{U_e S t} \tag{20}$$

L_{sep} (0.023 m), $\bar{a}_\delta$ (384.2 ms^{-1}) and U_e (1283.6 ms^{-1}) are evaluated from the mesh converged numerical solution to the eight degree flare case and St is assumed to be 0.01 [2, 3, 10]. Table 4 shows a comparison between the experimental surface pressure and heat-transfer establishment times compared to the wave and heat-transfer times. Surface-pressure establishment takes approximately 3.5 wave-times (t_w) to establish, while heat-transfer establishment times are approximately equal to the heat-transfer time (t_H). It is important to compare these factors to those found in other studies in the literature.

	Surface Pressure (ms)	Heat Transfer (ms)
Experimental	0.219	2.101
Analytical	0.060	1.790
Factor	3.650	1.175

Table 4: Experimental establishment times compared to their relevant analytical scaling parameters.

Figure 14 shows the ratio of experimental heat-transfer establishment time compared with the analytical heat-transfer time for various studies. Establishment times range from 0.037-1.175 t_H, showing that for any single experi-

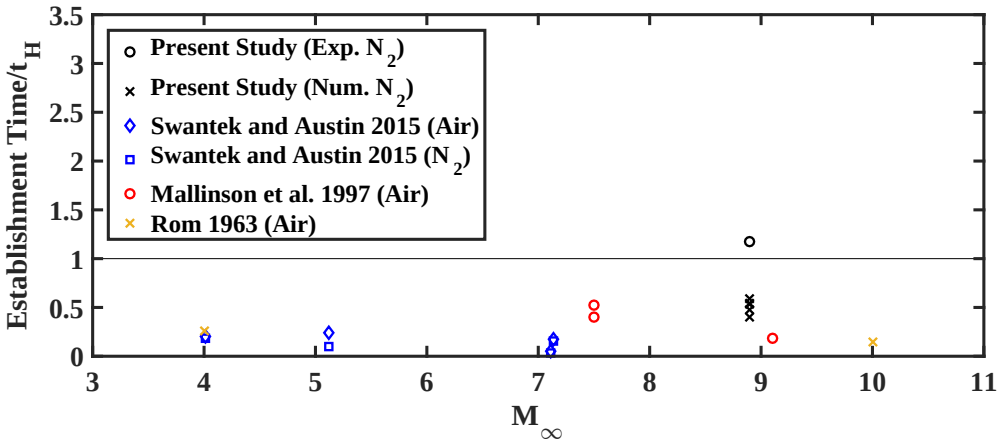

Figure 14: Experimental heat-transfer establishment time normalised by the heat-transfer time (t_H). Sources for data shown in legend. Black line shows y=1.

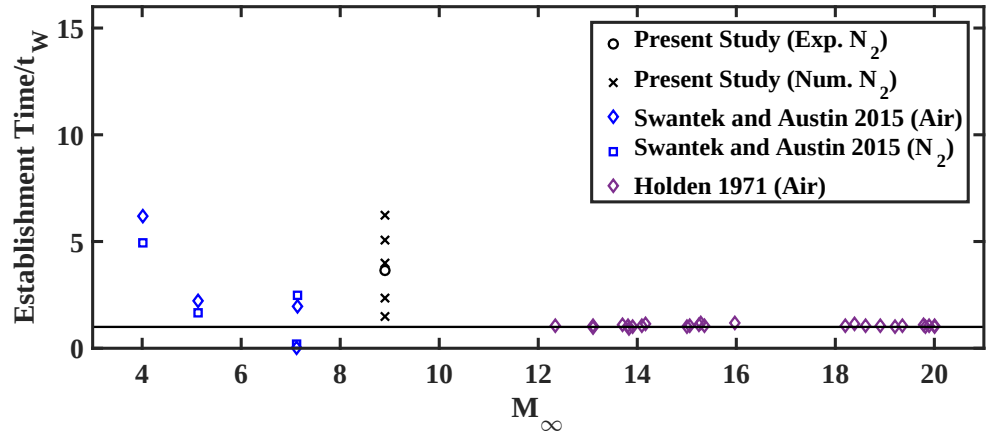

Figure 15: Experimental surface-pressure establishment time normalised by the wave-time (t_w). Sources for data in legend. Black line shows y=1.

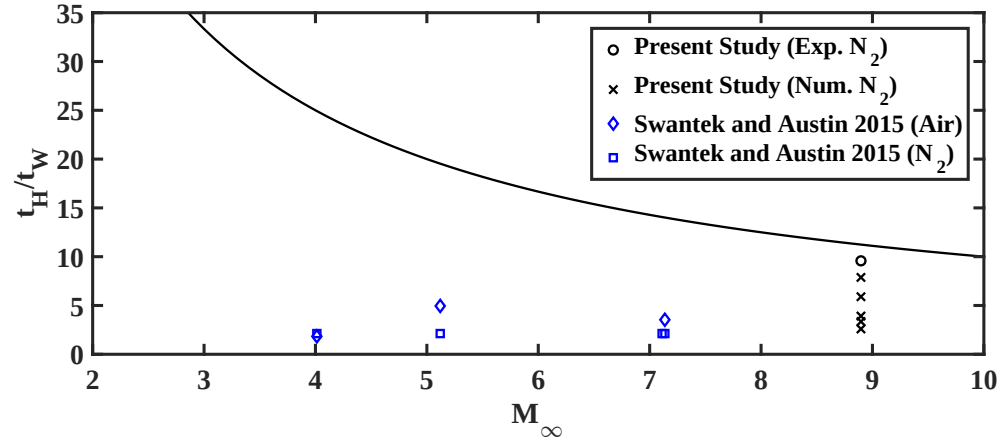

Figure 16: Ratio of experimental heat transfer and surface pressure establishment times. Sources in legend. Black line shows theoretical value according to equation 10.

ment the heat-transfer time does not seem to provide a consistent scaling for establishment. However, it does seem to provide a reasonable upper estimate for heat-transfer times, although at times, by a significant amount. It is also noted that for changing model geometry with the same conditions, the scaling of the heat-transfer establishment-time with heat-transfer time is not linear. As shown previously (figure 11 and figure 12) the separation length and numerical establishment times do not scale proportionally to each other. Hence, it is implied that there is some important geometry effect that this scaling does not account for. As will be shown, this is common for the other scaling parameters investigated here.

Figure 15 shows the ratio of the surface-pressure establishment times for various studies normalised by the analytical wave-time. Holden [1] finds that surface pressure establishment times are well approximated by the wave time. However when local Mach numbers are lower, considerable variation is introduced and the emergence of any strong trend is lacking. It is also noted that the surface-pressure establishment time scales poorly with the wave-time when conditions are held constant and model geometry changes. As with the heat-transfer, the reason for this is that the separation length and numerical establishment times do not scale proportionally with each other and hence a range of ratios is observed. Again, we see that this scaling parameter would likely be improved with some geometry factor.

As described by [3] in equation 10, the ratio of heat transfer to wave time should decrease with increasing Mach number, as shown by the black line in figure 16 which is asymptotic in nature. In a wider sense this concept could be expanded to ask if with very high Reynolds numbers (usually associated with high Mach numbers) is the establishment time also asymptotic, as the relative contribution of viscosity becomes increasingly negligible. It is noted that figure 15 does seem to show an asymptotic limit at high Mach number, although if the results of [1] are ignored this trend is less clear. For studies where estimates of both the experimental wave and heat transfer times are available this asymptotic scaling was investigated. Figure 16 clearly shows that experimental results do not follow the Mach scaling (equation 10) proposed by [3] and are instead relatively constant. Although, exactly how assumptions around the Stanton number required to simplify equation 9 to equation 10 could be affecting these results remains unclear.

It appears the relationship in equation 10 does not apply globally and sparse evidence exists for a Mach or Reynolds number dependence on convergence times. Again, part of this problem may well originate with the broad assumptions that must be made to relate different experiments and the lack of appropriate data on convergence times across different facilities.

C. Flow Length

As discussed earlier, Mallinson [6] suggest a different flow normalisation (equation 11) based on tunnel total enthalpy and the validity of this normalisation can be examined.

Data was extracted from figure 2 and additional data from other studies was compiled in order to produce figure 17. From this figure it is clear that the flow length ($l_f = t_{est}(2h_0)^{0.5}$) is also not a universal scaling parameter as no clear trend exists for all data points. This sort of normalization was unlikely to provide universal scaling as it does not

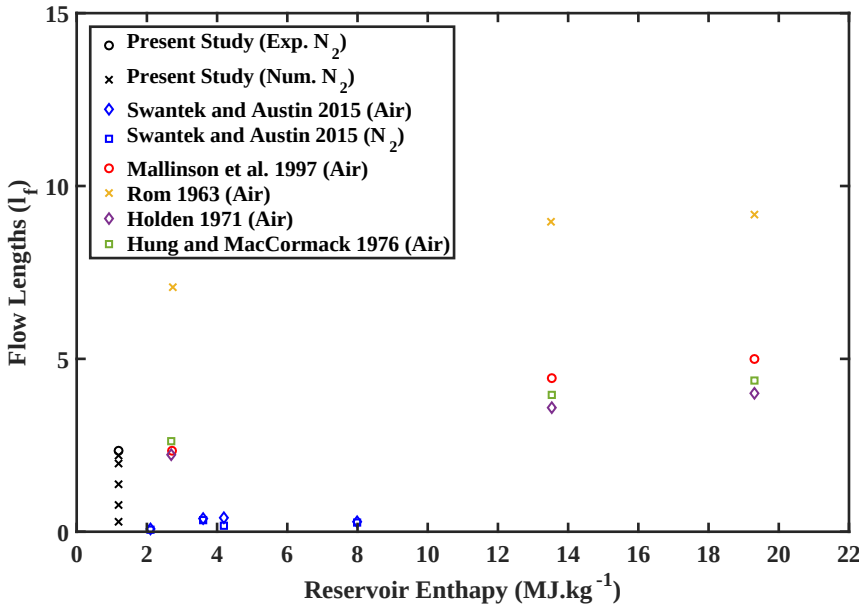

Figure 17: Establishment times of various experiments normalised using the flow length $(t_{est}(2h_0)^{0.5})$. Sources for data in legend.

rely on any local conditions. In fact, for high enthalpy facilities the flow length is physically similar to normalizing by flow time: $h_0 = C_pT + {}^1/_2U^2 \approx {}^1/_2U^2$ as $C_pT \ll {}^1/_2U^2$ and so in this limit the flow length (l_f) can be written as:

$$l_f \approx t_{est}(2[{}^1/_2{U_\infty}^2])^{0.5} \approx t_{est}U_\infty \tag{21}$$

If the flow length l_f is now divided by some characteristic length, such as the model length (L), then it is possible to recover the flow time normalization given in equation 1.

$$\frac{l_f}{L} \approx t_{est}\frac{U_\infty}{L} = \frac{t_{est}}{t_f} \tag{22}$$

Hence the normalisation proposed by [6] is approximate to the flow time but without normalisation by the model length. While this type of normalisation does not scale well globally, it does seem to scale well within certain 'families' of experiments. Here a family of experiments is considered as an experiment conducted in the same facility, with the same (or very similar) geometry at different flow conditions.

For instance, the establishment times seen at flow enthalpies of approximately 14 MJ kg^{-1} in figure 17 could be reasonably well approximated by linear extrapolation from the data in the same facilities at higher and lower flow enthalpies. This also suggests the flow time normalisation (equation 1) is also likely to provide an adequate scaling parameter within families of flows.

As seen with other scaling parameters, there is clearly some local geometry scaling that is not addressed, as shown

by the large scatter in the numerical results for different geometries from this study. Given the flow length scaling parameter includes no information on local conditions, this is not surprising.

VI. Possible Methods for Predicting Establishment Times

As many high-speed facilities are intermittent, the ability to accurately predict establishment of an experiment is important. However, assessing and comparing establishment times across many different studies is difficult. This problem is made considerably more complex by the lack of a consistent definition of establishment. A number of promising methods for scaling establishment have been investigated as well as direct prediction using numerical simulation. It is clear that none of the scaling parameters investigated is universal as no global trends are clear.

It is possible that many of the establishment metrics investigated would be significantly improved if some degree of geometry scaling parameter could be introduced. Indeed, none of the methods takes account of local factors, such as boundary-layer state, boundary-layer height, boundary-layer establishment times or mass scaling parameters, which have been shown by Souverein et al.[18] to be very important in the scaling of SWBLI. Potentially some form of mixed establishment metric could be formulated that includes both local and global parameters. Lack of available data means this is outside of the scope of this study. We wish to strongly encourage future studies to attempt to scale on these parameters, or atleast include details of these quantities in their papers to allow for meta-analysis.

Despite the lack of global trends a number of interesting results have emerged from the investigation of scaling parameters for the available data. The heat-transfer time proposed by Holden [1] appears to consistently over predict the heat-transfer establishment time (figure 14). Given that heat-transfer establishment time is always the limiting quantity, relative to surface pressure it might be reasonable to assume that an experiment is established in the time required to establish the boundary-layer plus the heat-transfer time. However, it should be noted that the heat-transfer time can over-predict reported establishment times by orders of magnitude. So while exceeding this criteria might indicate establishment, being under it does not mean that the experiment is not established.

The flow length seems to provide good scaling of establishment times within families of experiments. As seen in figure 17, flow length (equation 11) scales in a reasonably linear fashion with flow enthalpy when considering similar facilities and model geometries. If data is available for two very similar experiments at different flow enthalpies then it appears that establishment times can be reasonably interpolated over the range bounded by these results using this scaling (figure 16). However, this method appears to scale very poorly with changing model geometry and so comparison between models that are even moderately different should be avoided.

Numerical simulation was also investigated as a means for directly predicting establishment times. The lack of a common establishment criteria across experimental and numerical studies means that comparable data is very limited and so it is difficult to say with any confidence how accurate numerical predictions might be. For the single case investigated here, it appears that numerical simulation under predicts establishment times by approximately a factor of two. However, it is important to note that while experimental establishment times are larger they are also subject to

a series of weak waves that propagate through the test section which potentially inflate the establishment time relative to the numerical simulation. This highlights the importance of simulating the starting process of the tunnel as closely as possible. The establishment time of the numerical simulations is strongly dependent on it.

A hybrid method is suggested for assessing establishment times which depends on the amount of data available. In cases where the facility is new and little data is available for direct comparison with numerical simulation then the only way to confidently assess establishment is through a detailed study. This method is the most time consuming and expensive as it relies on experimental data. Potentially upper bounds of the establishment times can be assessed using the heat-transfer time, although with little data for comparison this method should be treated with care. Numerical simulation can be used to provide rough estimates of establishment times which ultimately require provisional studies in order to confirm.

In cases where a very different geometry is to be investigated but previous data is available, then numerical estimates of establishment are likely reasonable, but it is obviously important to validate numerical estimates from known experimental cases. This method is less expensive than conducting experiments, although at higher Mach numbers may not be possible due to limits on computational power. Also, heat-transfer times could be used again here, this metric is likely more useful when previous data is available for comparison. For cases where the model geometry is not changed significantly and the tunnel conditions will be changed then reasonable establishment estimates can likely be obtained from the flow length scaling.

VII. Conclusion

This study attempts to assess establishment times in intermittent high-speed facilities for separated SWBLI. Great variation is seen across the different experimental and numerical establishment times which has lead to a number of different metrics for their assessment. A number of these different scaling parameters were investigated: flow time, wave time, heat-transfer time and flow length. Unfortunately none of the scaling parameters investigated are capable of capturing enough of the driving physics of the flow to normalise well across all cases. A large part in the variation is likely due to a lack of any common establishment criteria in the literature.

This study serves as a benchmark case, as both experimental and numerical data were available for comparison. An establishment criteria was developed that showed reasonable agreement between experiment and simulation when compared to the range observed in the literature. It is important to note that in order to successfully compensate for variation between facilities some relative point must be chosen for comparison. The most appropriate quantity for selection appears to be establishment of the boundary-layer.

Of the scaling parameters investigated the type of scaling provided by these metrics can be broadly divided into two groups: local and global. Local scaling parameters (such as the wave or heat-transfer time) depend on conditions at the SWBLI but suffer from issues around a lack of accounting for establishment-time of the boundary-layer and so tend to scale poorly when comparing between facilities with different establishment times of the bulk flow and boundary-

layer. Global methods simply try to scale the establishment of the flow based on pertinent flow quantity(s) but ignore local conditions and so scale very poorly between experiments and tend to be the worse scaling parameter. Although, global methods do seem to provide a reasonable way of normalising between similar experiments in the same facility. Neither local or global scaling methods address changes in model geometry and these should be addressed with the most care.

This study does not address the differences between establishment in air compared with nitrogen. Nitrogen is less dissociative and hence non-equlibrium effect are less pronounced and little flow chemistry occurs. Many recent studies prefer to use nitrogen as a test gas as it simplifies the flow physics significantly. This is especially true of numerical studies where accurate non-equlibrium and chemical models are very hard to achieve. However, a switch to air will be required at some point, driven by a desire for more realistic data. This will be very challenging, our understanding of the driving flow physics must be improved significantly before the complicating effects of non-equilibrium, chemically reacting flows can be properly removed from the 'basic' underlying aerodynamics. However, should the reader wish to better understand how a change in test gas effects establishment times then Swantek et al. [11] likely provides some of the best information.

While a global scaling parameter was not evident, certain trends were observed from the data sets examined. The heat-transfer time proposed by Holden [1] appears to provide a reasonable upper bound on establishment times. Further, both flow length and flow time appear to provide a reasonable establishment time scaling parameter for families of studies. A number of scenarios are described where these scaling rules could be used.

Numerical simulations offer the most promising way of estimating establishment times. However, at such high Reynolds numbers it is often difficult or unfeasible to accurately simulate the entire model and the starting conditions of the experiment. For the single comparison made in this study, the numerical simulations appear to under-predict the experimental establishment times by a factor of two. However, it is difficult to know if this is inherent to the solver or simply due to differences in the way the experiment and simulation are started.

Successful design of a chosen test article is difficult. Ultimately, the only way to guarantee that an experiment is established is through thorough investigation of examined quantities during start-up and establishment of the tunnel flow. This approach is somewhat tedious and non-trivial (section III.B) and the temptation is to rely solely on numerical, analytical or empirical methods to justify establishment. As shown, there is no current global scaling parameter for estimating establishment times and as such this approach should be treated with care, even for similar facilities, conditions or geometries.

Acknowledgements

The authors would like to acknowledge S. Johnson, R. Hutchins and M.Grant for their technical expertise and support in running of the tunnel and model manufacture throughout this project. We would also like to acknowledge the Engineering and Physical Sciences Research Council (EPSRC) for supporting the present work through grant

EP/H020853/1.

References

[1] M. S. Holden. Establishment time of laminar separated flows. *AIAA Journal*, 9(11):2296–2298, nov 1971.

[2] Josef Rom. Measurements of heat transfer rates in separated regions in a shock tube and in a shock tunnel. *AIAA Journal*, 61(September), 1963.

[3] HK Ihrig and H Korst. Quasi-steady aspects of the adjustment of separated flow regions to transient external flows. *AIAA Journal*, 1(4):934–938, 1963.

[4] W. R. Davies and L. Bernstein. Heat transfer and transition to turbulence in the shock-induced boundary layer on a semi-infinite flat plate. *Journal of Fluid Mechanics*, 36(1):87–112, mar 1969.

[5] Roop N. Gupta. An Analysis of the Relaxation of Laminar Boundary Layer on a Flat Plate After Passage of an Interface with Application to Expansion-Tube Flows. Technical report, NASA, 1972.

[6] SG Mallinson, SL Gai, and NR Mudford. Establishment of steady separated flow over a compressioncorner in a freepiston shock tunnel. *Shock Waves*, pages 249–253, 1997.

[7] MC Druguet, GV Candler, and I Nompelis. Effects of numerics on Navier-Stokes computations of hypersonic double-cone flows. *AIAA journal*, 43(3), 2005.

[8] Datta V. Gaitonde, Patrick W. Canupp, and Michael S. Holden. Heat Transfer Predictions in a Laminar Hypersonic Viscous/Inviscid Interaction. *Journal of Thermophysics and Heat Transfer*, 16(4):481–489, oct 2002.

[9] Jean-Paul P. Davis and Bradford Sturtevant. Separation length in high-enthalpy shock/boundary-layer interaction. *Physics of Fluids*, 12(10):2661–2687, 2000.

[10] S. G. Mallinson, S. L. Gai, N. R. Mudford, Australian Defence, and Force Academy. The interaction of a shock wave with a laminar boundary layer at a compression corner in high-enthalpy flows including real gas effects. *Journal of Fluid Mechanics*, 342:1–35, jul 1997.

[11] a. B. Swantek and J. M. Austin. Flowfield Establishment in Hypervelocity Shock-Wave/Boundary-Layer Interactions. *AIAA Journal*, 53(2):311–320, feb 2015.

[12] CM M. CM Hung and RW W. RW MacCormack. Numerical solutions of supersonic and hypersonic laminar compression corner flows. *AIAA Journal*, 14(4):475–481, apr 1976.

[13] N. Murray, R. Hillier, and S. Williams. Experimental investigation of axisymmetric hypersonic shock-wave/turbulent-boundary-layer interactions. *Journal of Fluid Mechanics*, 714:152–189, jan 2013.

[14] I Nompelis, GV Candler, and M MacLean. Numerical investigation of double-cone flow experiments with high-enthalpy effects. *AIAA Paper*, 879(January), 2010.

[15] Leon Vanstone. *Shock-Induced Separation of Transitional Hypersonic Boundary Layers*. PhD thesis, Imperial College London, 2015.

[16] Ioannis Nompelis, GV Graham V Candler, and Michael S MS Holden. Effect of vibrational nonequilibrium on hypersonic double-cone experiments. *AIAA journal*, 41(11), 2003.

[17] J. Delery, J. G. Marvin, and Eli Reshotko. Shock-Wave Boundary Layer Interactions. Technical report, AGARD, 1986.

[18] L J Souverein, P G Bakker, and P Dupont. A scaling analysis for turbulent shock-wave / boundary-layer interactions. *Journal of Fluid Mechanics*, pages 505–535, 2013.

[19] D. Estruch-Samper, Leon Vanstone, B. Ganapathisubramani, R. Hillier, Leon Vanstone, and R. Hillier. Axisymmetric flare-induced separation of high-speed transitional boundary layers. In *50th AIAA Aerospace Meeting*, pages 1–14, 2012.

[20] D. Estruch-Samper, Leon Vanstone, B. Ganapathisubramani, and R. Hillier. Effect of roughness-induced disturbances on an axisymmetric hypersonic laminar boundary layer. In *51st AIAA Aerospace Sciences Meeting*, pages 1–11, 2013.

[21] S. G. Mallinson, R. Hillier, A.P. Jackson, D.C. Kirk, S. Soltani, and M. Zanchetta. Gun tunnel flow calibration: defining input conditions for hypersonic flow computations. *Shock Waves*, 10(5):313–322, nov 2000.

[22] Donald Lorimer Schultz and T. V. TV Jones. Heat-Transfer Measurements in Short-Duration Hypersonic Facilities. *AGARD*, 1973.

[23] HGL. Dragonfly DF24F Seriese Datasheet, 2014.

[24] R. Hillier, D. Kirk, and S. Soltani. Navier-Stokes computations of hypersonic flows. *Internation Journal of Numerical Heat & Fluid Flow*, 1995.

[25] G Strang. On the Construction and Comparison of Difference Schemes. *Journal on Numerical Analysis*, 5(3):506–517, 1968.

[26] Matania Ben-Artzi and Joseph Falcovitz. A second-order Godunov-type scheme for compressible fluid dynamics. *Journal of Computational Physics*, 55(1):1–32, 1984.

[27] R J Stalker. A study of the free-piston shock tunnel. *AIAA Journal*, 5(12):2160–2165, 1967.

[28] R. A. East, R. J. Stalker, and J. P. Baird. Measurements of heat transfer to a flat plate in a dissociated high-enthalpy laminar air flow. *Journal of Fluid Mechanics*, 97(1980):673, 1980.